Laser-assisted charge transfer in positronium collisions with protons and antiprotons

H. B. Ambalampitiya

Quantemol Ltd., 320 City Rd, London EC1V 2NZ, UK
and Department of Physics and Astronomy,
University of Nebraska, Lincoln, Nebraska 68588-0299, USA

J. Stallbaumer and I. I. Fabrikant

Department of Physics and Astronomy,
University of Nebraska, Lincoln, Nebraska 68588-0299, USA

(Dated: April 1, 2022)

Abstract

We study the process of laser-assisted charge transfer in collisions of positronium atoms with protons (antiprotons) with formation of Rydberg hydrogen (antihydrogen) atoms by the use of Classical Trajectories Monte Carlo simulations of Ps-p dynamics in a linearly polarized infrared field. We do not observe a drastic enhancement of the cross sections similar to that predicted before in laser-assisted electron bremsstrahlung and electron recombination since in the present charge transfer process the Coulomb focusing effect is absent. Still we see a substantial enhancement up to a factor of three in the energy range between 10^{-4} and 0.1 eV for the field of intensity between 10 MW/cm^2 and 10 GW/cm^2. The effect depends weakly on the orientation of the incident Ps velocity relative to the field polarization vector. Rydberg states of the produced hydrogen atoms whose orbits are close to circular can survive against ionization by laser field and decay spontaneously to lower states. This is favorable for spectroscopic studies of antihydrogen atoms.

I. INTRODUCTION

Control of atomic processes by external fields is one of the most interesting aspects of atomic physics important for various applications. In particular electron collisions with positive ions can be strongly influenced by laser fields of a moderate intensity. The Coulomb-focusing effect [1] has been shown to enhance the cross sections and rates for several low-energy electron collision processes: bremsstrahlung, radiative recombination and dissociative recombination [2–4]. In the present paper we investigate how a laser field of a moderate intensity (of the order of 10 MW/cm^2 - 10 GW/cm^2) can influence the charge transfer processes

$$\text{Ps}(n_{\text{Ps}}l_{\text{Ps}}) + p \rightarrow \text{H}(n_{\text{H}}l_{\text{H}}) + e^+$$

$$\text{Ps}(n_{\text{Ps}}l_{\text{Ps}}) + \bar{p} \rightarrow \bar{\text{H}}(n_{\bar{\text{H}}}l_{\bar{\text{H}}}) + e^-.$$

The second process is important for antihydrogen studies [5–15]. In fact it is considered now as one of the most efficient ways of antihydrogen creation. To be specific we will be discussing the first process of the hydrogen formation, but due to the charge conjugation symmetry all results will equally apply to the second process.

In contrast to the processes of laser-assisted radiative and dissociative recombinations, in the present process the electron is initially bound, therefore it is unlikely that the Coulomb focusing effects would play a role. On the other hand, due to the wiggling motion of a charged particle in an ac field, it seems probable that the external field can enhance or suppress the electron transfer from Ps to proton.

A complete quantum treatment of the charge transfer is a very challenging task even in the absence of external fields. It involves very sophisticated two-center close coupling calculations [16–18] which turn out to be also very time-consuming because they require inclusion of many Ps states and H states to achieve convergence. However, several comparisons [19–22] of quantum and classical calculations for zero field have shown that the Classical Trajectory Monte Carlo (CTMC) simulations agree very well with the quantum-mechanical convergent close coupling calculations [16–18] if the incident Ps atom is in an excited state, and the agreement improves with the growth of n_{Ps}, in accordance with the generalized correspondence principle [23]. This can be explained by the dominance of the long-range interaction between the Ps atom in the excited state and the proton [18]: due to the degeneracy of Ps states with different orbital angular momenta the effective interac-

2

tion between the excited Ps and the proton is effectively dipolar [24], and scattering by the dipolar potential is similar in classical and quantum mechanics [21]. In the present study we have extended the CTMC method to the charge transfer process in an external laser field with the incident Ps atom in an excited state. Previous classical [25, 26] and quantum [27–29] calculations of laser-assisted hydrogen/antihydrogen formation in Ps collisions with protons/antiprotons typically involve Ps in the ground state and relatively high field intensities and collision energies. For example calculations of Lévêque-Simon and Hervieux [29] were carried out for the field 10^7 V/cm in the range of antiproton energies from 4 to 10 keV corresponding to the center-of-mass energy in the range from 2.2 to 5.4 eV. In the present paper we focus on the fields of much lower strength (between 10^5 and 2.5×10^6 V/cm) and much lower center-of-mass energies relevant to Ps collisions in antiproton traps [8, 11, 30, 31]. The considered fields are nevertheless high enough for a possible ionization of antihydrogen after its formation. These aspects of the problem are also discussed in the present paper. Atomic units are used throughout unless stated otherwise.

II. DESCRIPTION OF THE METHOD

The theory of CTMC for a three-body system consisting of charged particles where two of them are bound is described in refs. [23, 32]. The CTMC approach has been applied before in the case of a Ps atom interacting with a proton with no external laser field [19–22]. In the laser-assisted case, the theory is described in brief as follows. For a given impact parameter and the principal quantum number n_{Ps} of the projectile Ps atom, an ensemble of initial states is prepared by a random selection of the eccentricity, the orientation of the mutual motion (Kepler orbits) of the $e^- - e^+$ pair, and the position of e^- on the orbit. A classical trajectory for each random state is then propagated towards the proton which is stationary at the origin of the configurations space. The dynamics of the system is governed by the following time-dependent Hamiltonian.

$$H(q, p, t) = \sum_{i=1}^{6} \frac{p_i^2}{2} - \frac{1}{|\mathbf{q}_{e^-}|} + \frac{1}{|\mathbf{q}_{e^+}|} - \frac{1}{|\mathbf{q}_{e^-} - \mathbf{q}_{e^+}|} - \mathbf{F}(t) \cdot (\mathbf{q}_{e^+} - \mathbf{q}_{e^-}), \qquad (1)$$

where (q, p) collectively represent the set of coordinates and momenta of the electron and the positron, and $\mathbf{F}(t)$ is the time-dependent electric field. The interaction with the laser field is considered in the dipole approximation. In what follows, we assume the laser is

3

linearly polarized along an arbitrary direction indicated by the polarization vector $\mathbf{e}$ which makes an angle θ with the initial center-of-mass velocity of Ps. The time dependence of the electric field is then given by

$$\mathbf{F}(t) = \mathbf{e}F\cos(\omega t + \phi_0) \qquad (2)$$

where F, ω and ϕ_0 are the amplitude, angular frequency, and the initial phase of the field, respectively.

The Hamiltonian in Eq. (1) is solved using the regularization method described in [33, 34]. The solutions are propagated giving sufficient time for the interaction with the target and the laser field. At the end of the propagation, the final energies and the angular momenta of the trajectories are checked to generate the statistics in different final channels to calculate the probabilities and cross sections. For example, the charge-transfer probability $P(b)$ as a function of the impact parameter b is computed as a ratio between the number of trajectories leading to the formation of the final atom and the total number of sampled trajectories. The charge-transfer cross section σ_{CT} is then given by the integral $\int 2\pi P(b) b db$. The total number of trajectories for each energy point was varied between 6×10^4 and 10^6 to make sure that the statistical error for the cross section is less than 1%. Like in our previous calculations [2–4] we average results for the cross section over ϕ_0 which is equivalent to averaging over the position of Ps when it enters the field region. If the Ps velocity is randomly oriented, like in traps, then the cross section should be also averaged over the angle θ between the polarization vector and the initial Ps velocity vector. The sensitivity of the final results to the parameters F, ω, ϕ_0 and θ will be discussed in the following sections.

III.   RESULTS AND DISCUSSION

We have calculated laser-assisted charge transfer (LACT) in the field range between 0.2×10^{-4} and 5×10^{-4} a.u. corresponding to intensities between 14.0 MW/cm² and 8.77 GW/cm², and frequencies ω from 0.01 a.u. to 0.1 a.u. corresponding to the laser wavelength ranging from 4.6 μm to 0.46 μm. The initial n_{Ps} was varied from 2 to 6, and the cross sections were averaged over l_{Ps}. In Figs. 1 and 2 we present cross sections summed over l_H and n_H for $n_{Ps} = 4$ and 6 in the range of Ps energies between 0 and 1 eV which is virtually the same as the center-of-mass energy. The energy range from 10^{-2} to 10^{-1} eV is relevant to present
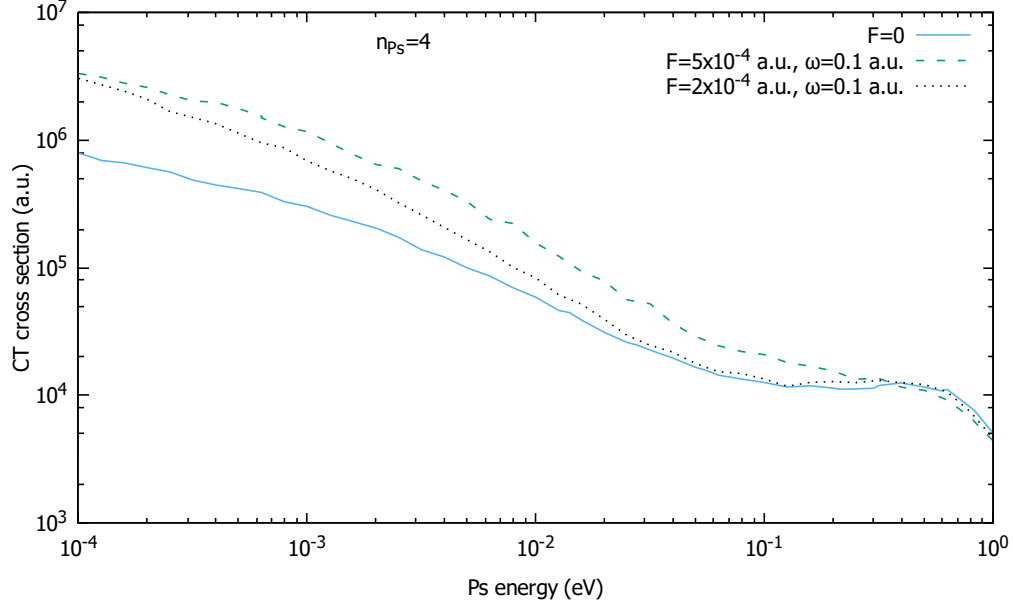
FIG. 1. Charge transfer cross section for $n_{\mathrm{Ps}} = 4$, $\phi_0 = 0$, $\theta = 0$. Values of F and ω are indicated in the legend.
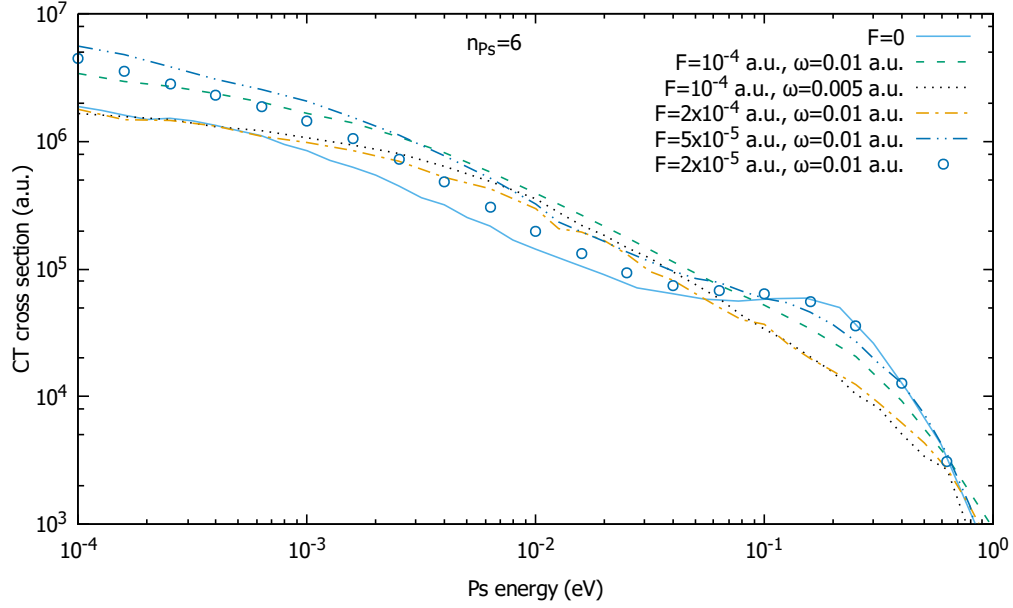

FIG. 2. The same as in Fig. 1 for $n_{\mathrm{Ps}} = 6$.

experiments.

In the low-energy region a substantial enhancement, by a factor 2-3, of the charge transfer is observed, although at higher energies the field may lead to the cross section suppression. To investigate the origin of the enhancement, in Figs. 3 and 4 we present the charge transfer
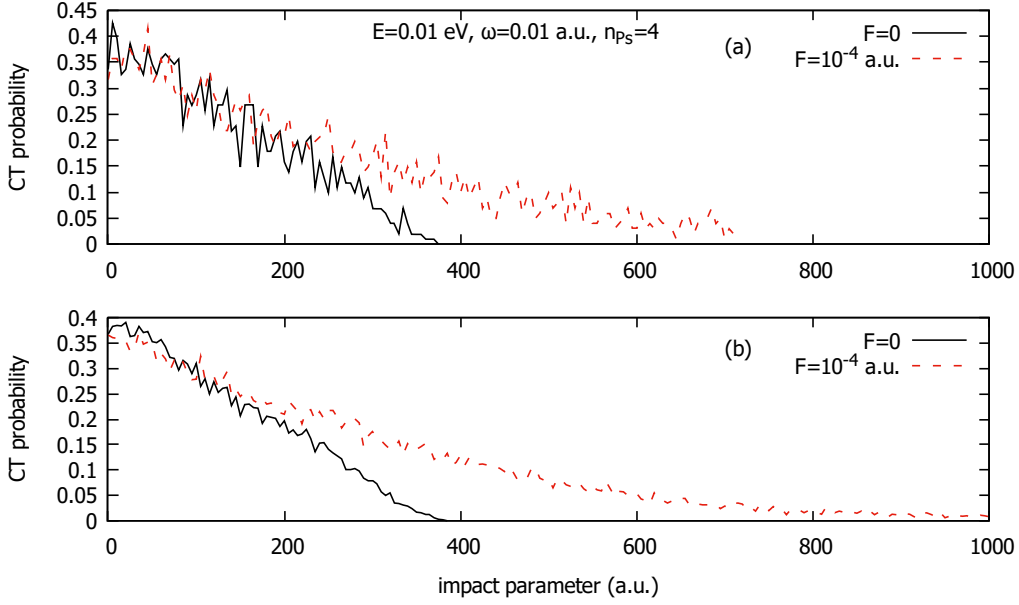
FIG. 3. Charge transfer probability as a function of impact parameter for collision energy $E = 0.01$ eV, $n_{\mathrm{Ps}} = 4$, comparison of zero-field and nonzero-field cases. Panel (a): $N_{tr} = 100$, panel (b): $N_{tr} = 1000$.

probability P as a function of the impact parameter b for the collision energy $E = 0.01$ eV. The fluctuations in the function $P(b)$ represent statistical uncertainties in CTMC calculations. To show how they are reduced with the increase of number of trajectories N_{tr} for each impact parameter, we present $P(b)$ for two values of N_{tr}, 100 and 1000. The statistical uncertainty is about 20% in the first case, and about 5% in the second. Note, however, that the uncertainty is substantially lower in cross sections which are calculated from much larger number of trajectories. In the considered examples the LACT probability remains nonzero in much larger range of the impact parameters than the zero-field probability. This explains the cross section enhancement in the low-energy region observed in Figs. 1 and 2. However, this enhancement is very sensitive to the collision energy. At lower energies the probability at nonzero fields is reduced at lower impact parameters. This is illustrated in Fig. 5 which shows that at $E = 10^{-4}$ eV the probability for nonzero field is substantially lower than for zero field for impact parameters below 1800 a.u. This leads to approximately the same value of the cross section at this energy for $F = 0$, 10^{-4} and 2×10^{-4} a.u. shown in Fig. 2.

Therefore, in contrast to electron recombination processes, the field-induced enhancement is not universal, but depends on the field parameters, the Ps energy and the initial state of
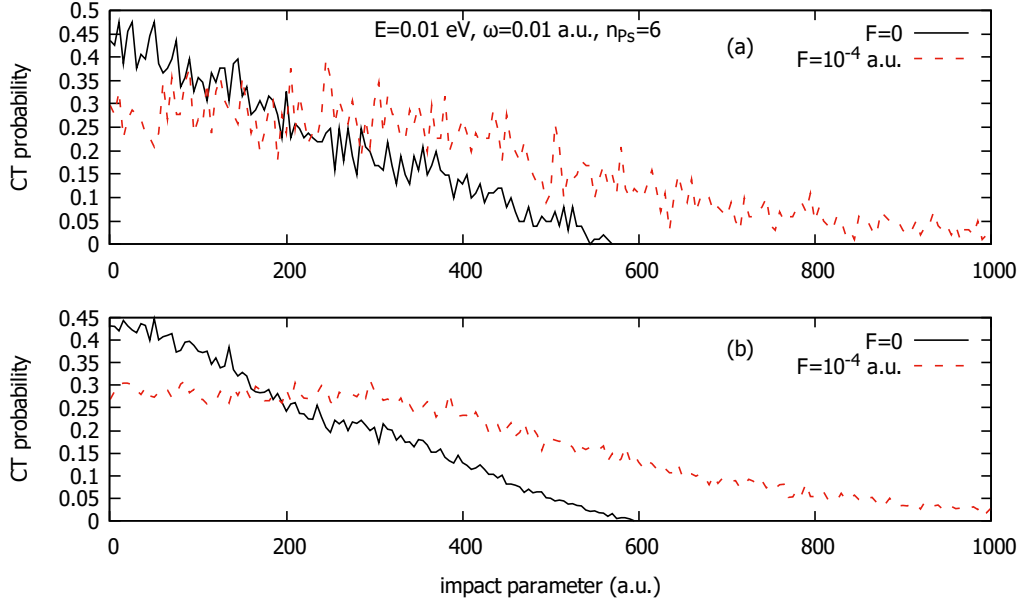
6

FIG. 4. The same as in Fig. 4 for $n_{\mathrm{Ps}} = 6$,. Panel (a): $N_{tr} = 100$, panel (b): $N_{tr} = 1000$.
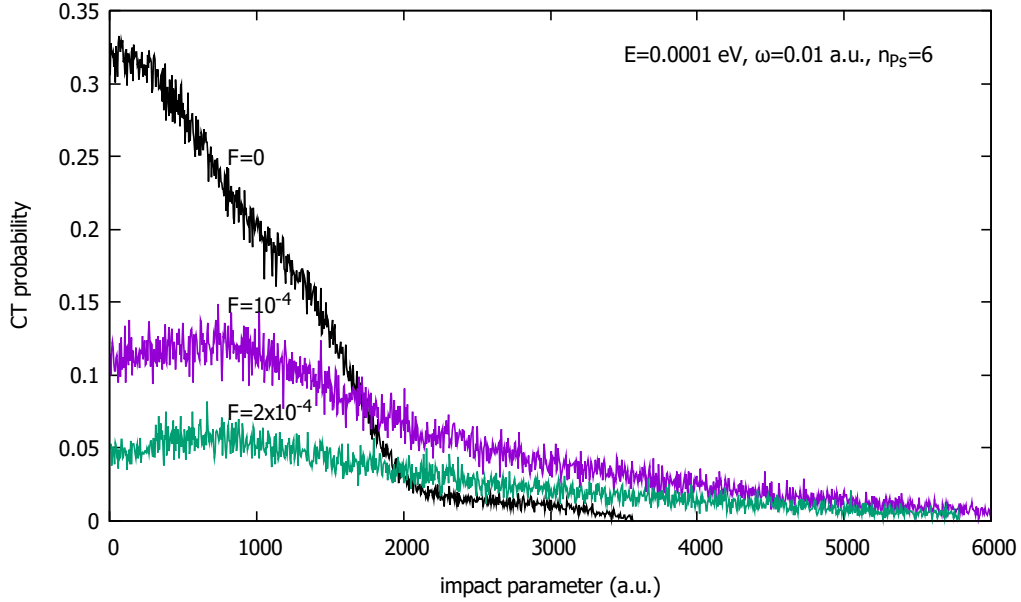

FIG. 5. Charge transfer probability as a function of impact parameter for collision energy $E = 10^{-4}$ eV, $n_{\mathrm{Ps}} = 6$, comparison of zero-field and nonzero-field cases ($N_{tr} = 1000$).

Ps. To demonstrate how the field influences the charge transfer processes, in Figs. 6 and 7 we present typical electron trajectories for higher impact parameters for zero and nonzero fields. In both cases the field stimulates the charge transfer which is absent for nonzero fields. It is apparent though that there is no systematic enhancement in the present case,
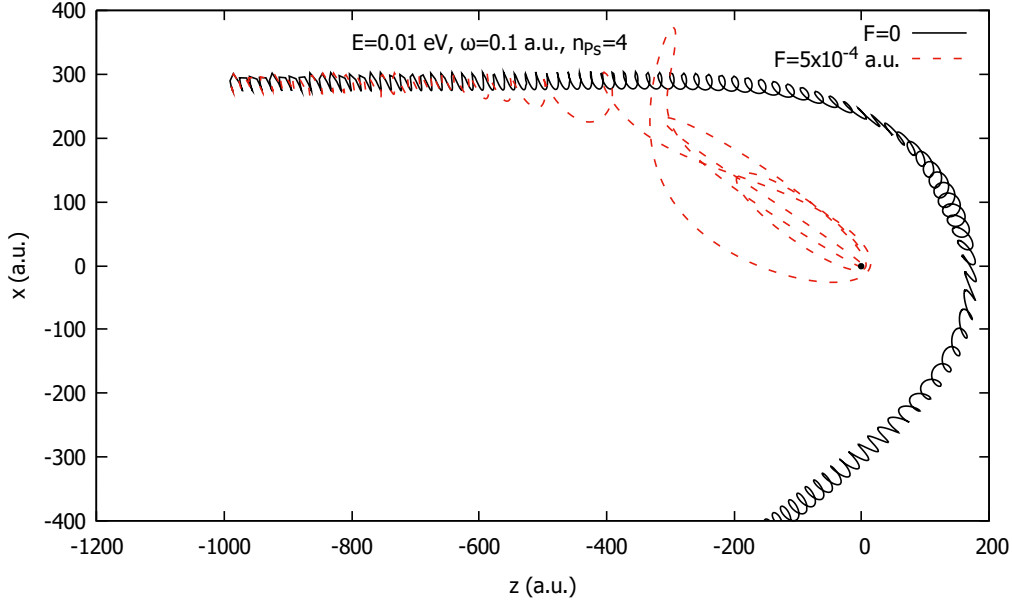
7

FIG. 6. Projection of electron trajectories on xz plane for $E = 0.01$ eV, impact parameter $b = 300$ a.u., $n_{Ps} = 4$. The position of the proton at the origin is indicated by a filled circle. The field is along z axis, and the initial conditions (chosen randomly) are the same for both trajectories.

like in the case of charged-particle collisions [2–4] when the cross section enhancement is due to the Coulomb focusing. A relevant observation is the absence of chaos in the present problem. This is in contrast with the problems involving electron-proton interaction [2–4] where the probability of the process depends randomly on the impact parameter due to the chaotic nature of the Hamiltonian combining the Coulomb interaction and interaction with the laser field [35, 36]. In the present case $P(b)$ dependence is regular except numerical uncertainties discussed above.

Another interesting feature in the present case is a very low sensitivity of the cross section to the phase ϕ_0. In the case of charged-particle collisions, in particular in laser-assisted radiative recombination process, the cross section is very sensitive to ϕ_0 due to the dependence of the electron drift velocity on ϕ_0, and peaks very sharply at two values of ϕ_0. In the present case calculations show that the cross section is very weakly dependent on ϕ_0. Our results are also insensitive to the angle θ between the laser polarization vector and the initial velocity vector. This again is different from the case of electron collisions. All calculations presented in the figures were carried out for $\theta = 0$, but additional calculations carried out for several values of theta between 0 and π do not exhibit a significant difference
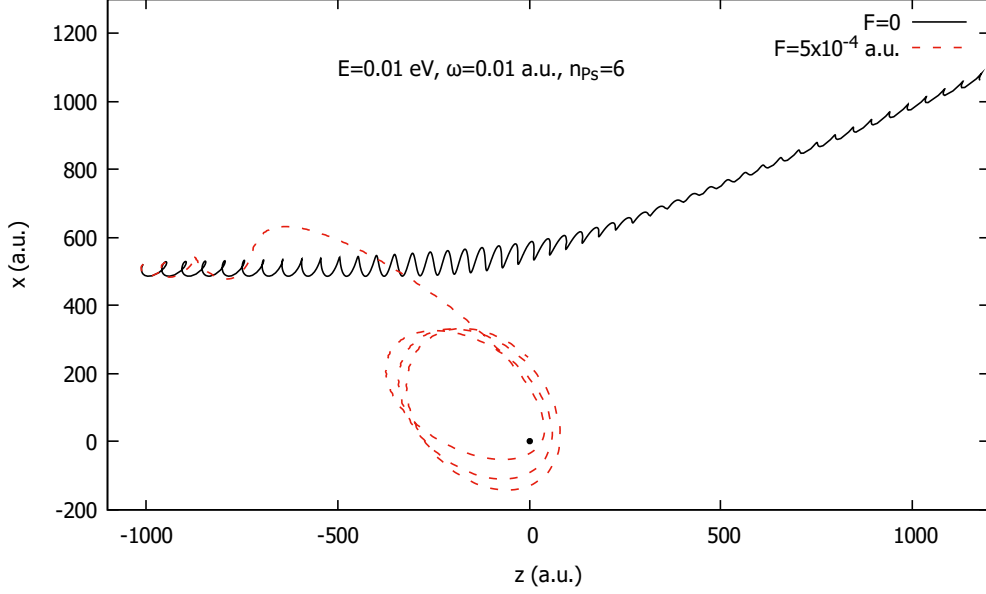
8

FIG. 7. The same as in Fig. 6 for impact parameter $b = 500$ a.u., $n_{\mathrm{Ps}} = 6$.

with the $\theta = 0$ case.

In Figs. 8 and 9 we show the final-state distribution in n_{H}, i.e. partial LACT cross sections as functions of n_{H}. For the zero field the H production is sharply peaked at the value of n_{H} approximately satisfying the resonance condition, as was earlier observed in [19],

$$n_{\mathrm{H}} = n_{\mathrm{Ps}}\sqrt{2}.$$

Typically the resonance charge transfer occurs in collisions between heavy particles [37] because of the low probability of the energy exchange between the nuclear and electron motions, but the previous [19] and present calculations for the charge transfer in the Ps-p collisions show that even for collisions involving a light particle (Ps) the resonance charge transfer is highly likely. However, the field broadens n_{H} distribution substantially. Typically the increase of intensity leads to a broader distribution, but also lower field frequencies lead to the broadening as well. Both effects are associated with exchange energy between the field and one or both of the light particles, electron and positron. The field-induced broadening strongly reduces the cross section at the resonant peak, but it allows production of the H atom in highly excited states.
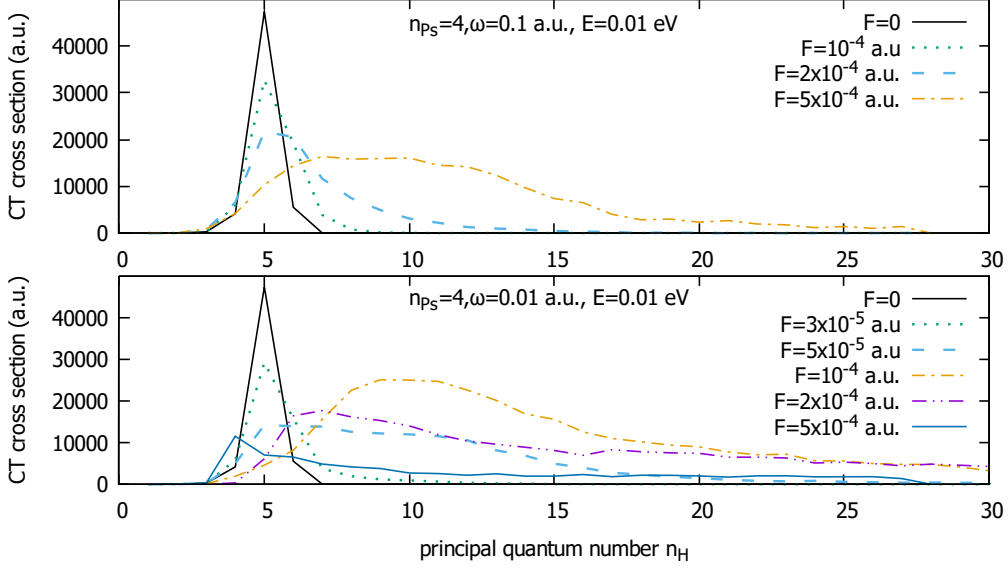
9

FIG. 8. Partial cross section as a function of n_{H} for $E = 0.01$ eV, $n_{\mathrm{Ps}} = 4$ for a few sets of field parameters.

IV. DECAYS

A state formed during the charge transfer is subject to decay due to two possible processes: photoionization due to the laser field and transitions to lower states due to spontaneous emission. The latter process is favorable for the purpose of creation of antihydrogen atoms, however its rate decreases fast with the growth of n_{H}. Although the photoionization rate decreases as well, for a typical value of n_{H} and low l_{H} the photoionization rate is significantly higher than the spontaneous decay rate. For example, for $F = 10^{-4}$ a.u., $\omega = 0.1$ a.u., $n_{\mathrm{H}} = 7$, $l_{\mathrm{H}} = 1$ the photoionization rate

$$W_{\mathrm{PI}} = \frac{I}{\hbar\omega}\sigma_{\mathrm{PI}}$$

is 0.790×10^{-8} a.u.$=0.327$ ns^{-1} whereas the spontaneous decay rate is 3.7×10^{-10} a.u.$=0.015$ ns^{-1}. In the equation above I is the field intensity, and σ_{PI} is the photoionization cross section.

In Fig. 10 we compare photoionization rate for $F = 10^{-4}$ a.u., $\omega = 0.1$ a.u. and spontaneous emission rate. Note that in all considered cases the Keldysh parameter is high, therefore tunneling ionization can be neglected. All rates are averaged over initial l_{H} and summed over final electron orbital angular momentum. The calculations have been carried
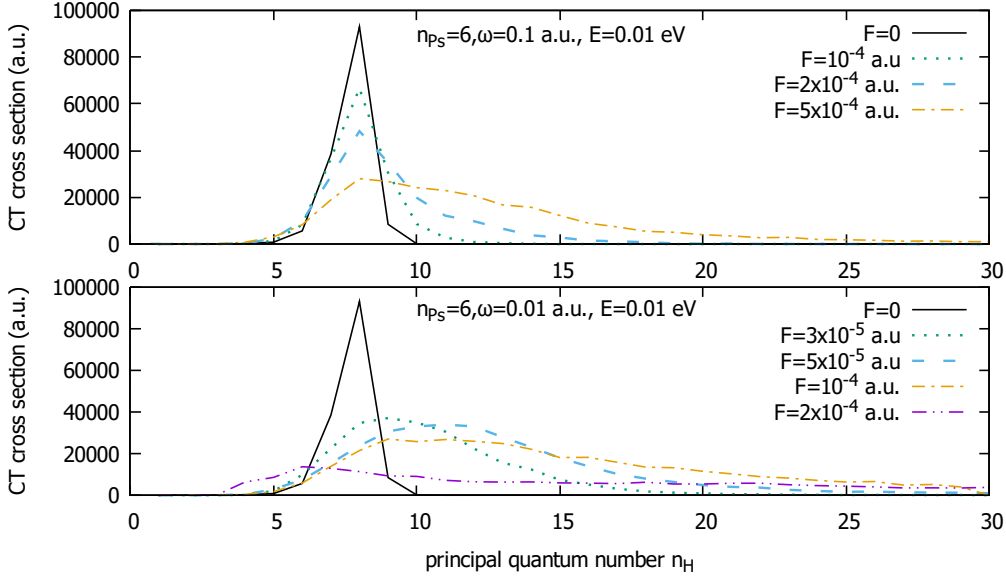
10

FIG. 9. Partial cross section as a function of n_H for $E = 0.01$ eV, $n_\mathrm{Ps} = 6$ for a few sets of the field parameters.

out according to the Gordon's formulae [38, 39] for photoionization and spontaneous emission formulae of Bethe and Salpeter [40]. Although the photoionization rate decays with n_H like n_H^{-5} [41], slightly faster than the spontaneous emission rate, $n_\mathrm{H}^{-4.5}$ [40], even at $n_\mathrm{H} = 20$ the photoionization rate is still an order of magnitude higher than the spontaneous emission rate. The field increase leads to a further increase of photoionization rate as F^2 until it reaches the tunneling regime where the rate increase becomes exponential. Moreover, the reduction of the frequency with the aim to increase the field effect in the charge transfer, also leads to strong increase of photoionization rates. Finally, the states which are not ionized by one photon, for example $n_\mathrm{H} = 7$ at $\omega = 0.01$ a.u., can be ionized by two-photon processes. An estimate based on the semiclassical equation [42] for the two-photon ionization shows that in the listed example the two-photon ionization rate still exceeds spontaneous emission rate.

However an analysis of the final-state distribution in l_H produces a more favorable outcome. An inspection of classical trajectories shows that many electron orbits produced as a result of the charge transfer have rather low eccentricities consistent with the fact that external fields efficiently mix different l and m states within a given n manifold. In Fig. 11 we show l_H distributions for different values of n_H. Note that since these are classical simu-
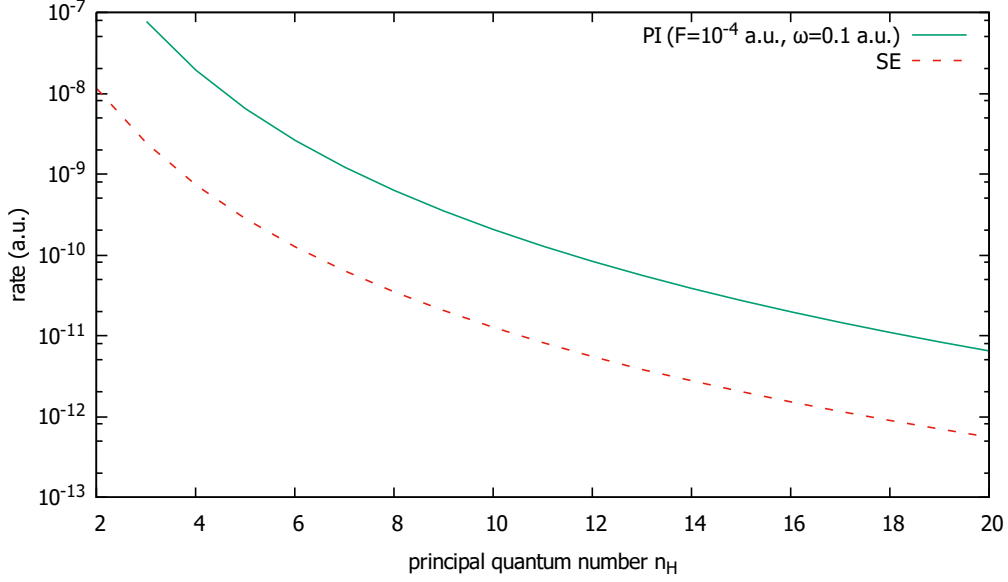
FIG. 10. Comparison of photoionization rate for typical values of F and ω (upper curve) and spontaneous emission rates as functions of n_{H}.

lations, they produce nonzero results for $l_{\mathrm{H}} = n_{\mathrm{H}}$ corresponding to circular orbits. Generally contribution of events with l_{H} close to n_{H} is substantial. Moreover, according to Fig. 11, contribution of orbits with higher l_{H} is somewhat growing with the increasing energy. Such orbits have very low photoionization rates. Moreover, the decrease of photoionization rate with l_{H} is substantially faster than the decrease of the spontaneous emission rates.

In Fig. 12 we compare photoionization rate and spontaneous emission rate as functions of l_{H} for two values of n_{H}. The photoionization rate drops much sharper and crosses the spontaneous decay curve below $l_{\mathrm{H}} = 6$. Therefore we conclude that external laser field would be efficient in production of excited states with low eccentricity, that is with l_{H} close to n_{H}. Since the photoionization rate for these states is very low, a spontaneous radiative decay of these states can be observed. This gives an opportunity to do antihydrogen spectroscopy of excited states with the help of the LACT in Ps-$\bar{p}$ collisions.

V. CONCLUSION

Most calculations of laser-assisted electron collisions are performed quantum-mechanically (see [3] and references therein) which is challenging computationally and typically involves
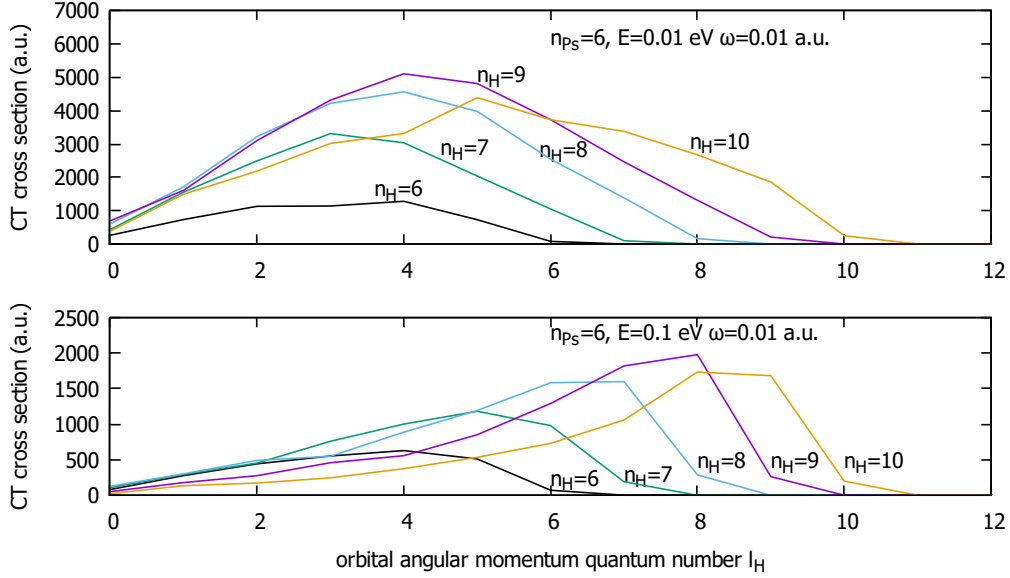
FIG. 11. Final l_H distributions for $F = 10^{-4}$ a.u., $\omega = 0.01$ a.u. and two Ps energies, $E = 0.01$ and 0.1 eV.

approximations, like the strong-field approximation. However low-energy collisions involving Coulomb interaction can be treated classically provided that the Coulomb parameter $q_1 q_2 / \hbar v$ is large [43] where q_1, q_2 are charges of interacting particles, and v is their relative velocity. Similarly, collisions involving hydrogen-like systems in excited states also can be treated classically with a good accuracy because of the dominance of dipolar force [21, 22]. We have taken advantage of this observation to perform CTMC calculations of LACT in collisions of Ps with protons with the results equally valid for Ps-$\bar{p}$ collisions. The influence of the laser field in this case is not as dramatic as in collisions involving electron-proton interaction [2–4] because of the absence of the Coulomb focusing effect in the present case. There is also no chaotic behavior in the present problem like that observed for the Hamiltonian involving the combination of the Coulomb and laser fields. Still, in the low-energy region between 0.1 and 100 meV it is possible to increase the charge-transfer cross section by a factor of three with the field of intensity as low as 14 MW/cm^2. The analysis of the decay of the formed H($n_H l_H$) atoms show that states with higher l_H close to n_H, or orbits close to circular, can survive against photoionization due to the external field and decay spontaneously with the rates higher than photoionization rates. This give an opportunity to do spectroscopy of excited antihydrogen atoms formed in the process of charge transfer in Ps-antiproton collisions.
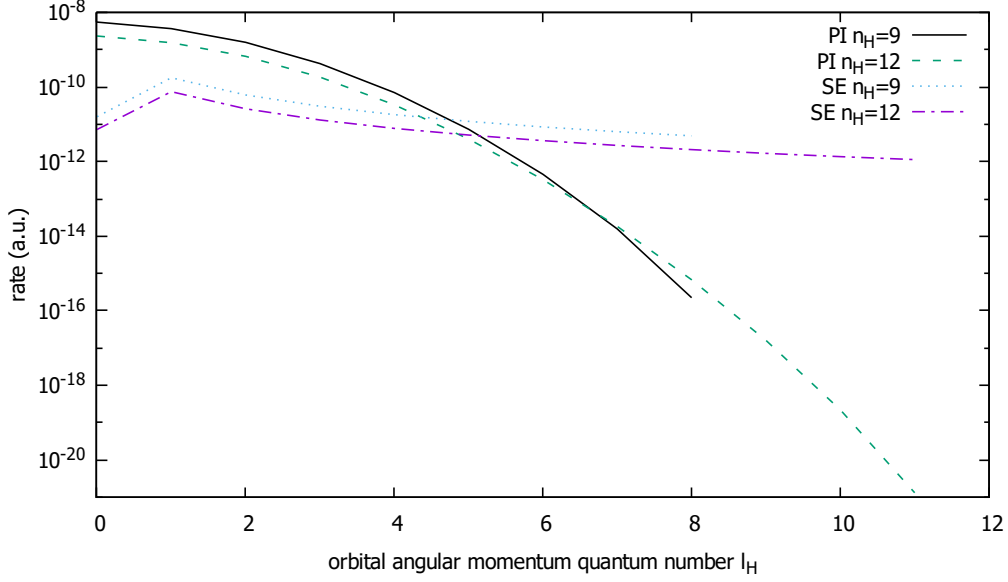
13

FIG. 12. Comparison of photoionization rates (curves PI) and spontaneous emission rates (curves SE) as functions of l_H for $F = 10^{-4}$ a.u., $\omega = 0.1$ a.u.

---

[1] Th. Brabec, M. Yu. Ivanov, and P. B. Corkum, Phys. Rev. A **54** R2551 (1996).

[2] H. B Ambalampitiya and I. I. Fabrikant, Phys. Rev. A **99**, 063404 (2019).

[3] I. I. Fabrikant and H. B Ambalampitiya, Phys. Rev. A **101**, 053401 (2020).

[4] I. I. Fabrikant, H. B Ambalampitiya, and I. F. Schneider, Phys. Rev. A **103**, 053115 (2021).

[5] M. Charlton, Phys. Lett. A **143**, 143 (1990).

[6] B. I. Deutch, M. Charlton *et al.* Hyperfine Interact. **76**, 153 (1993).

[7] J. P. Merrison, H. Bluhme, J. Chevallier, B. I. Deutch, P. Hvelplund, L. V. Jørgensen, H. Knudsen, M. R. Poulsen, and M. Charlton, Phys. Rev. Lett. **78**, 2728 (1997).

[8] Storry C H *et al.* (ATRAP Collaboration), Phys. Rev. Lett. **93**, 263401 (2004).

[9] P. Scampoli and J. Storey, Modern Physics Letters A **29**, 1430017 (2014).

[10] S. Aghion *et al.* (AEgIS Collaboration), Phys. Rev. A **94** 012507 (2016).

[11] W. A. Bertsche, E. Butler, M. Charlton, and N. Madsen, J. Phys. B **48**, 232001 (2015).

[12] W. A. Bertsche, Phil. Trans. Royal Soc. A: Math. Phys. Eng. Sciences **376**, 20170265 (2018).

[13] M. Charlton, S. Eriksson, and G. M. Shore, *Antihydrogen and fundamental physics* (Springer, 2020) pp. 1-95.

[14] C. Amsler *et al.*, Communication Physics **4**, 19 (2021).

[15] B. H. Kim *et al.*, Acta Physica Polonica A **137**, 122 (2020).

[16] A. S. Kadyrov and I. Bray, Phys. Rev. A **66**, 012710 (2002).

[17] A. S. Kadyrov, C. M. Rawlins, A. T. Stelbovics, I. Bray, and M. Charlton, Phys. Rev. Lett. **114**, 183201 (2015).

[18] A. S. Kadyrov, I. Bray, M. Charlton, and I. I. Fabrikant, Nature Commun. **8**, 1544 (2017).

[19] D. Krasnicky, R. Caravita, C. Canali and G. Testera, Phys. Rev. A **94**, 022714 (2016).

[20] D. Krasnicky, G. Testera, and N. Zurlo, J. Phys. B **52**, 115202 (2019).

[21] H. B. Ambalampitiya, D. V. Fursa, A. S. Kadyrov, I. Bray, and I. I. Fabrikant, J. Phys. B **53**, 155201 (2020).

[22] M. Charlton, H. B. Ambalampitiya, I. I. Fabrikant, D. V. Fursa, A. S. Kadyrov, I. Bray, Phys. Rev. A **104**, L060803 (2021).

[23] R. Abrines and I. C. Percival, Proc. Phys. Soc. **88**, 873 (1966).

[24] M. Gailitis and R. Damburg, Proc. Phys. Soc. **82**, 192 (1963).

[25] R. J. Whitehead, J. F. McCann, and I. Shimamura, Phys. Rev. A **64**, 023401 (2001).

[26] J. S. Cohen, Phys. Rev. A **67**, 017401 (2003).

[27] A. B. Voitkiv, B. Najjari, and J. Ulrich, J. Phys. B **35**, 2205 (2002).

[28] A. Chattopadhyay and C. Sinha, Phys. Rev. A **74**, 022501 (2006).

[29] K. Lévêque-Simon and P.-A. Hervieux, J. Phys. Conf. Series **1412**, 222007 (2020).

[30] E. A. Hessels, D. M. Homan and M. J. Cavagnero, Phys. Rev. A **57**, 1668 (1998).

[31] F. Castelli, I. Boscolo, S. Cialdi, M. G. Giammarchi, and D. Comparat, Phys. Rev. A **78**, 052512 (2008).

[32] I. C. Percival and D. Richards, Adv. At. Mol. Phys. **11**, 1 (1976).

[33] S. J. Aarseth and K. Zare, Celestial Mechanics **10**, 185 (1974).

[34] H. B. Ambalampitiya, <u>Semiclassical methods in atomic and molecular physics</u>, PhD Thesis (2021).

[35] L. Wiesenfeld, Phys. Lett. A **144**, 467 (1990).

[36] L. Wiesenfeld, Acta Phys. Polonica B **23**, 271 (1992)

[37] J. B. Delos, Rev. Mod. Phys. **53**, 287 (1981).

[38] W. Gordon, Ann. d. Phys. **2**, 1031 (1929).

[39] A. Burgess, Memoirs of the Royal Astronomical Society, **69**, 1 (1965).

[40] H. A. Bethe and E. Salpeter, *Quantum Mechanics of One and Two-Electron Atoms.* Springer, Berlin, 1957.

[41] H. A. Kramers, Philos. Mag. **46**, 836 (1923).

[42] I. Berson, Phys. Lett. A **84A**, 364 (1981).

[43] L. D. Landau and E. M. Lifshitz, *Quantum Mechanics (Nonrelativistic Theory)* (Pergamon, Oxford, 1977).